Proceedings of the 20th International Conference on Soil Mechanics and Geotechnical Engineering– Rahman and Jaksa (Eds)

Experimental study of failed drilled shafts' residual capacity

Étude expérimentale de la capacité résiduelle d'un puits foré défaillant

Anne Lemnitzer & Rabie Farrag
Dept of Civil & Environmental Engineering, University of California, Irvine, 4135 Eng. Gateway, Irvine, CA, USA, alemnitz@uci.edu

Carter Cox
Bridge Engineer, HDR Inc, Irvine, CA, USA

Ben Turner
Senior Engineer, Dan Brown and Associates, San Luis Obispo, CA, USA

ABSTRACT: Lateral large-scale testing of two pile specimens with a diameter of 0.46m and a total length of 4.57m was performed up to complete structural failure. The piles were embedded in 1.83m of loose backfill sand with a relative density of 20%. At the tip, the piles were embedded in 1.22m of simulated rock. The piles reached an ultimate capacity (P_{ult}) near 72kN at a corresponding pile head displacement of 20cm. Post-test soil excavation around the piles was used to document pile damage and crack propagation. The analytically predicted shear failure did not occur; rather, a flexure-triggered failure through the formation of a plastic hinge above the rock-socket was observed. Following test completion and failure documentation, additional soil was placed with the same technique to raise the fill height above the rock socket from 1.83m to 3.05m. The test setup allowed for re-testing of the damaged pile specimen, which is rarely possible in practice. Retesting allowed for studying the magnitude of residual capacity of the damaged pile and assessing soil resistance independent of the pile as the pile was previously loaded to failure. Retesting with 64% more soil compared to the original soil thickness provided an additional 80% capacity compared to P_{ult} of the damaged specimen.

RÉSUMÉ : Des essais latéraux à grande échelle de deux spécimens de pieux d'un diamètre de 0,46 m et d'une longueur totale de 4,57 m ont été effectués jusqu'à la défaillance structurelle complète. Les pieux ont été enfoncés dans 1,83 m de sable de remblai meuble avec une densité relative de 20 %. A l'extrémité, les pieux étaient encastrés dans 1.22m de roche simulée. Les pieux ont atteint une capacité ultime (Pult) proche de 72kN à un déplacement de tête de pieu correspondant de 20cm. L'excavation du sol après l'essai autour des pieux a été utilisée pour documenter les dommages aux pieux et la propagation des fissures. La rupture par cisaillement prévue par l'analyse ne s'est pas produite ; on a plutôt observé une rupture déclenchée par la flexion par la formation d'une charnière plastique au-dessus de l'embase rocheuse. Après l'achèvement de l'essai et la documentation de l'échec, de la terre supplémentaire a été placée avec la même technique pour augmenter la hauteur de remplissage au-dessus de l'emboîtement rocheux de 1.83m à 3.05m. Le montage de l'essai a permis de tester à nouveau le spécimen de pieu endommagé, ce qui est rarement possible dans la pratique. Ce nouvel essai a permis d'étudier l'ampleur de la capacité résiduelle du pieu endommagé et d'évaluer la résistance du sol indépendamment du pieu, ce dernier ayant été précédemment chargé jusqu'à la rupture. Le ré-essai avec 64% de sol en plus par rapport à l'épaisseur originale du sol a fourni une capacité supplémentaire de 80% par rapport à Pult du spécimen endommagé.

KEYWORDS: lateral load test, pile foundations, plastic hinge, pile failure, cyclic loading

1 INTRODUCTION

Earthquake reconnaissance efforts, e.g., following the 1999 Izmit, Turkey earthquake, or the 2010 Maule, Chile earthquake, have demonstrated that pile foundations are highly susceptible to severe damage during strong ground shaking. Drilled shafts are common deep foundation elements used in bridges and other structures to support applied axial and lateral loading resulting from self-weight, live loads, and extreme loads, such as wind, earthquakes, water current, or lateral impacts. Since an inelastic pile response may be difficult to avoid under strong earthquake loading, post-yield performance of pile foundations, and particularly inelastic deformations, become critically important to the global foundation and superstructure performance. Most commonly the pile integrity is compromised by the formation of a plastic hinge which, depending on the soil properties, forms between 2-4 pile diameters below ground surface. The relationship between the plastic hinge location and soil-pile system was first presented by Priestly *et al*. 1996, based on the work of Budek *et al*. 1994. Priestly *et al*. suggested that the pile plastic hinge location is a function of pile diameter, the pile's above-ground cantilever height, and the subgrade reaction modulus. Chai and Hutchinson (2002) further demonstrated that the plastic rotation capacity was greatly improved by the external confinement provided by the surrounding soil.

This study investigates experimentally the drilled shaft integrity of two pile specimens following simulated earthquake loading up to ultimate structural capacity. It then assesses the residual pile capacity, the load redistribution, and the relocation of the piles' plastic hinges through ground modification, i.e., the modification of the in-situ soil stratigraphy by addition of supplemental fill material.

Specifically, two pile specimens were laterally loaded under reverse cyclic loading up to complete structural failure (plastic hinge developed), then retested after adding 4ft [1.2m] of sand surcharge. The added sand layer was intended to reduce the above-grade cantilever height of the specimen and to provide supplemental external confinement, which in return relocated the plastic hinge to a higher elevation and provided an intermittent pile surplus capacity. This rapid "repair" method has significant potential as a short-term post-earthquake stability increase of pile foundations since it does not involve intensive excavation or cure time for concrete repair work.

2 EXPERIMENTAL PROGRAM

2.1 *Test Configuration*

The experimental studies were executed in the "soil pit" at the Structural Engineering Testing Hall of the University of California, Irvine. Two test specimens named Specimen 2 and Specimen 3 were embedded in a constructed sand-over-rock stratigraphy and tested in two sequential phases (hereafter referred to as Phase 1 and Phase 2). Phase 1 was part of an experimental investigation of rock-socketed drilled shafts, which evaluated the development and magnitude of shear stresses at the soil-rock interface and their impact on the pile failure development (Farrag *et al.*, 2020). In Phase 1, the pile specimens were subjected to reverse cyclic lateral loading until complete structural failure was reached, i.e., a plastic hinge formed above the rock-socket. Following test completion, the pile specimens were retested (Phase 2) under the same loading protocol; however, a sand layer of 4ft [1.2 m] thick was added in an attempt to (1) identify potential post-test residual capacities, (2) strategically relocate the plastic hinge developed in Phase 1 to a higher elevation, and (3) separate the contribution of soil resistance from the overall pile capacity in an attempt to better understand the soil structure interaction behavior of the foundation-soil system. Pile specimens were identical in geometry, soil stratigraphy, and longitudinal reinforcement; however, varied in the transverse reinforcement ratio. Specimens 2 and 3 had transverse reinforcement volumetric ratio of 0.95% and 0.23% respectively. Figure 1 shows schematics of the specimen configurations and soil stratigraphy during testing in Phase 1 and Phase 2.

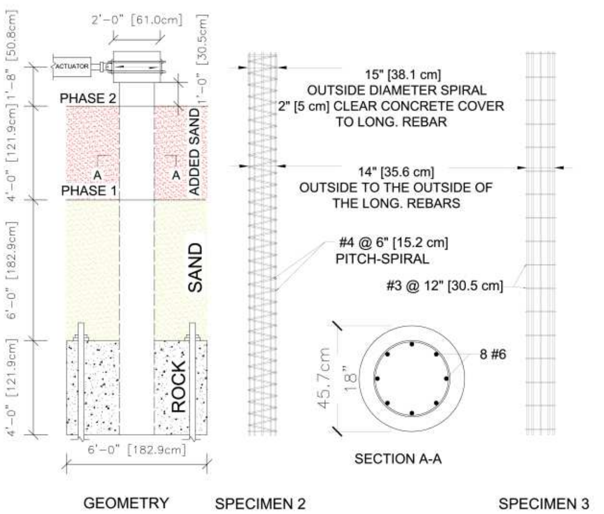

Figure 1. Schematic specimens' configuration and soil stratigraphy

2.2 *Material Properties*

2.2.1 *Pile Materials*

The tested piles consisted of reinforced concrete piles. Upon instrumenting the rebar cages, the concrete piles were precast. Concrete cylinders with dimensions of 15 cm [6 in] in diameter by 30.5 cm [12 in] in height were taken on site per ASTM C39. Pile Specimens 2 and 3 had a 28-day design compressive strength of 27.58 N/mm2 [4 ksi], and cylinder break strengths of 39.3, and 39.3 MPa [5.7, and 5.7 ksi] on the day of testing, respectively. The average Young's modulus obtained from the concrete cylinders' stress-strain curves was 26.6 GPa [3856 ksi].

2.2.2 *Soil and Rock Material*

The sand material was selected based on local availability. Over one dozen fill materials from different suppliers were evaluated in the laboratory. The sand material chosen to be used in this study had a friction angle of 38 deg determined through direct shear testing per ASTM D3080, and a maximum dry unit weight of 21 kN/m^3 [134 pcf] determined via modified Proctor compaction testing (ASTM D1557). The sand material was pluviated from a fixed drop height that was always maintained in order to achieve a uniform density profile throughout. In situ undisturbed samples were collected during the pluviation process and the average measured relative density was 20%. The low in-situ relative density of 20% provided a strong stiffness contrast between the soil and simulated rock. A similar contrast can be found between very soft clays (e.g., San Francisco bay mud) and underlying rock formations. This strong stiffness contrast was needed in Phase 1 of the testing program, where shear magnitudes at the stiffness boundaries were investigated (Farrag *et al.*, 2020). Extensive laboratory and in-situ testing were performed to characterize the fill material. CPT and DMT testing was performed before and after testing. Test results are omitted for brevity. The rock layer was experimentally simulated by high-strength concrete. The simulated rock concrete had a 28-day design compressive strength of 34.5 MPa [5ksi], and an average cylinder break strength of 48.3 MPa [7ksi] on the day of testing.

2.3 *Specimen Instrumentation*

Specimens were instrumented with external and internal sensors including linear voltage differential transducers (LVDT), string potentiometers (SP), inclinometers, and strain gauges in longitudinal (E/W) directions. Also, external strain gauges arranged in rosette configuration were placed on the exterior concrete surface of the pile (R). A schematic instrumentation plan for Specimen 2 is shown in Figure 3.

2.4 Pile installation

The two pile specimens were constructed as follows: First, the rebar cages were instrumented and placed into temporary pile formwork (Sonotubes). After concrete was placed and cured (approximately one week), a pile cap was constructed. The pile caps were used to attach the actuator and apply lateral loading to each pile. Along the socket lengths of the piles (1.22 m [4 ft]) from the bottom, the pile surfaces were scarified with a pneumatic needle scaler to improve adherence between the "rock concrete" and the pile, and to better replicate the rough interface typical for a drilled rock socket. Following the curing of the piles, they were centered and secured inside the rock socket form work and the block of concrete was poured. The soil was placed in the soil pit by dry pluviation and leveled upon reaching the design height for phase 1 (see Figure 4a). This overall construction sequence is opposite of regular in situ construction procedures in which a drilled shaft is cast in a drilled hole, but was utilized here for convenience and to allowed for careful specimen construction without damaging the extensive instrumentation network. Following phase 1 completion and after failure investigation, soil material was placed back into the excavated areas around the piles, and additional soil was placed with the same technique to raise the fill height above the rock socket from 1.83m to 3.05m (see Figure 4c).

2.5 *Load Application*

The pile lateral-load test was performed on the two test piles in two stages, with the first stage aimed to degrade the pile stiffness and reach structural failure, and the second stage intending to improve the soil stratigraphy, ultimately aiming to restore the pile capacity. The lateral loading protocol was developed based on the predictive analyses and followed the general guidelines of the ASCE 41-17 (2017) recommendations in which applied lateral displacement levels are selected as fractions or multipliers of the anticipated yield displacement. Loading was applied under displacement control at the center of the pile cap using a 76.2-cm [30-in] stroke, 667-kN [150-kip] capacity hydraulic actuator (see Figures 3 and 5). Phase 1 loading protocol included three cycles per displacement level up to ultimate capacity. Hereafter, two cycles per displacement level were performed until substantial degradation of the lateral load-displacement relationship due to plastic hinge creation was noticeable. The loading protocol for Phase 2 included only one cycle per each displacement level, as shown in Figure 5.

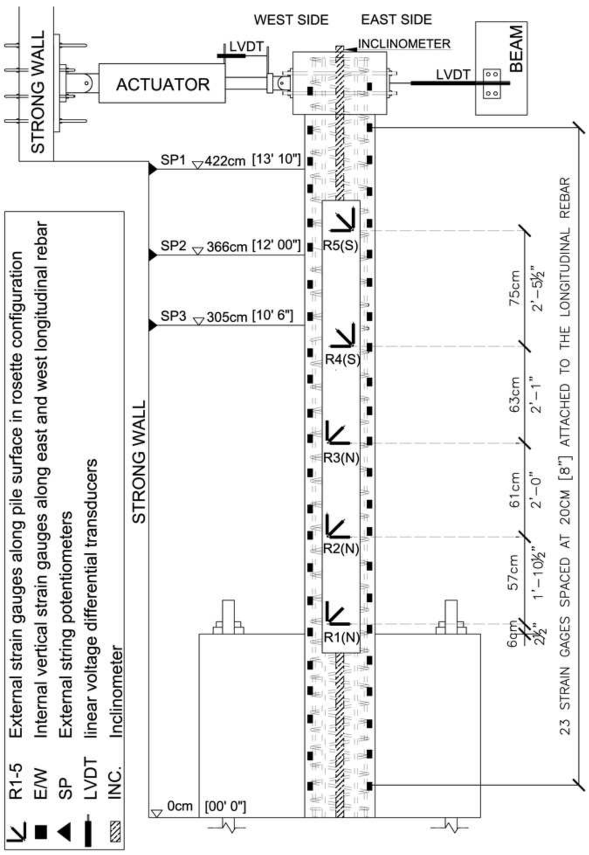

Figure 3. Instrumentation layout for Specimen 2

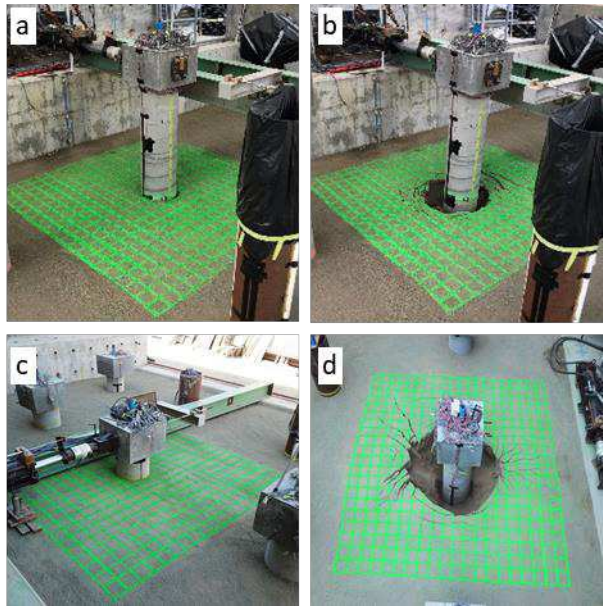

Figure 4. (a) before and (b) after initial testing (Phase 1) of Specimen 2, and (c) before and (d) after retesting of Specimen 2 (Phase 2).

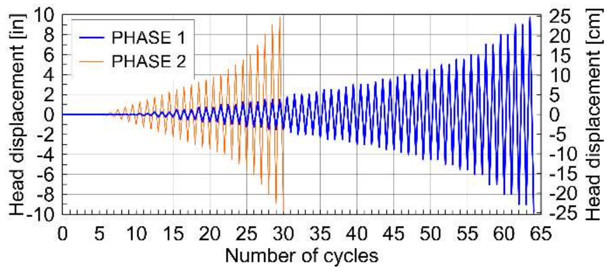

Figure 5. Pile head displacement history and loading cycles for Phase 1 and 2

3 EXPERIMENTAL RESULS

3.1 Observations

A spray-painted grid with dimensions of 15 x 15 cm [6 x 6 in] was applied to the sand surface around the pile specimen to monitor the extents of soil cracking, heaving, and caving. As depicted in the photographs of Figure 4 and 6, circumferential crack expansion and the formation of “crater-type” holes around the piles at lateral displacements larger than 10 cm [4 in] occurred during both the initial testing and the retesting. The soil collapse at the ground level around the pile could be attributed to the compaction and caving of the relatively loose sand under the large cyclic lateral loading. Upon the test completion the soil was excavated on the west side of Specimen 2 and the crack pattern shown in Figure 6 was observed. Cracks above the preexisting plastic hinge region cracks were observed after Phase 2 providing an evidence of a plastic hinge relocation. It was also noted that the cave-in and subsequent recompression of the soil affected the response of the pile-soil interaction in a way that it moved the point of maximum moment (aka, plastic hinge) higher.

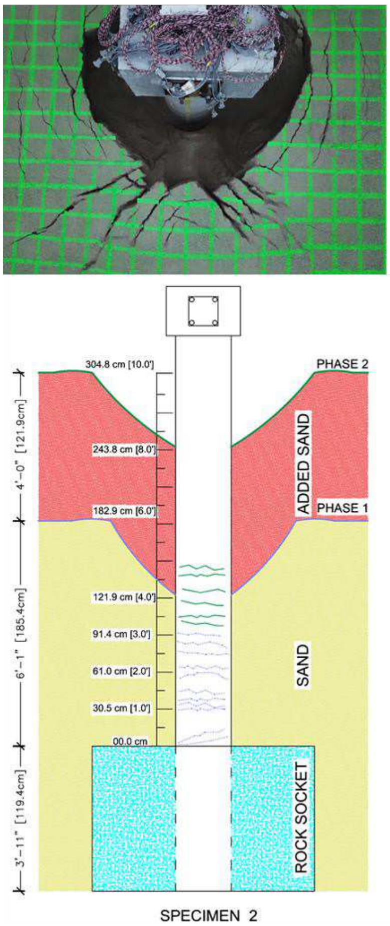

Figure 6. Major cracks along the pile depth and around the surface soil at test completion of Specimen 2

3.2 *Load Displacement Relationships*

Phase 2 load-displacement responses of Specimens 2 and 3 are compared to their initial test responses (Phase 1) in Figures 7 and 8. The backbone curve of Specimen 2 suggests that the retested pile specimen was able to reestablish the same initial pile-soil system stiffness. After adding the soil fill, Specimen 2's lateral load capacity increased by approximately 80% in both, pull and push directions. The retested Specimen 2 also showed higher ductility in comparison to its initial testing (Phase 1). On the other hand, Specimen 3 was able to restore about 60% of its initial pile-soil stiffness. The retested Specimen 3 also showed higher ductility in comparison to the initial testing. This reduced initial stiffness during Phase 2 testing is a result of Specimen 3 having minimal transverse reinforcement, and therefore, the residual stiffness after the initial testing was lower than that of Specimen 2. The Specimen 3 lateral load capacity was increased by about 84% in push- and 59% in pull directions comparison to capacities reached during Phase 1 testing.

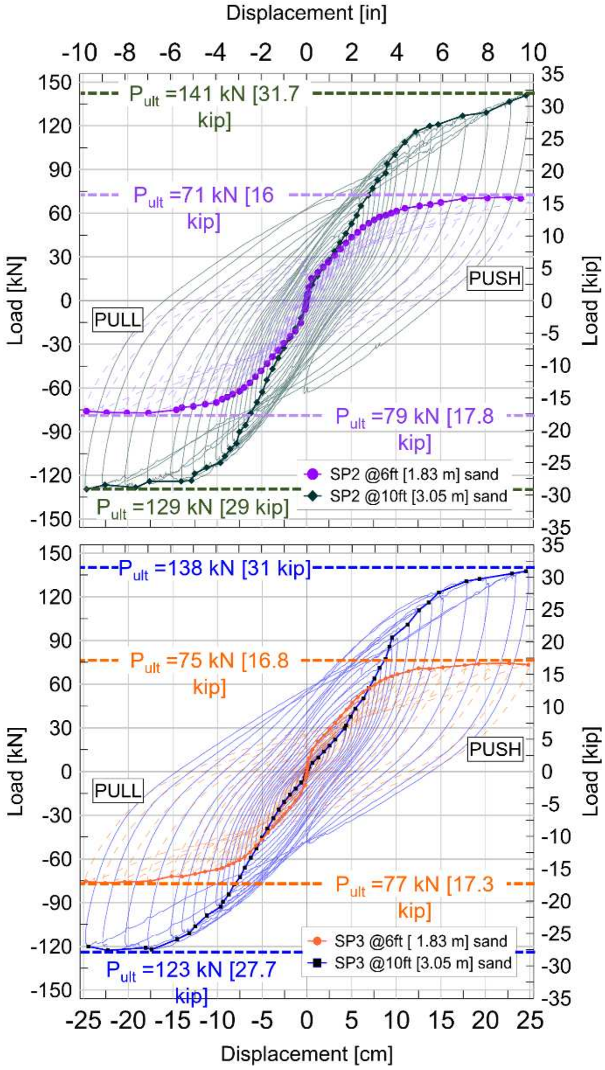

Figure 7. Experimental load-displacement relationships with backbone curves of Specimens 2 and 3.

The magnitude of plastic deformations (△ plastic) for a certain cycle can be calculated as the difference in displacement at zero pile head load (e.g., intersection of the load deformation curve with x-Axis) as shown in Figure 8. Specimens 2 and 3 had an accumulated plastic deformation of 0.9 in [2.3 cm] at lateral pile head displacement of 4 in [10 cm] during Phase 1, and 1.8 in [4.6 cm] during Phase 2 as shown in Figure 8. Both retested specimens had a 100% increase in their plastic deformation. The increase in plastic deformation can be explained by a new plastic hinge being developed as an extension to the preexisting plastic hinge from Test 1. Also, the higher plastic deformations experienced in the retested piles contributes to the stiffness recovery when cracks are closed during displacements imposed in the other direction, which ultimately contributes to the increase in the observed lateral load capacity. It was also noted that the stiffness of the retested piles degraded at a slower rate than that of the initial test (Phase 1). The energy dissipation during each cycle can be calculated from the enclosed area within the hysteresis loop as illustrated in Figure 8. The energy dissipation of the retested piles was approximately double the energy dissipated during Phase 1 testing.

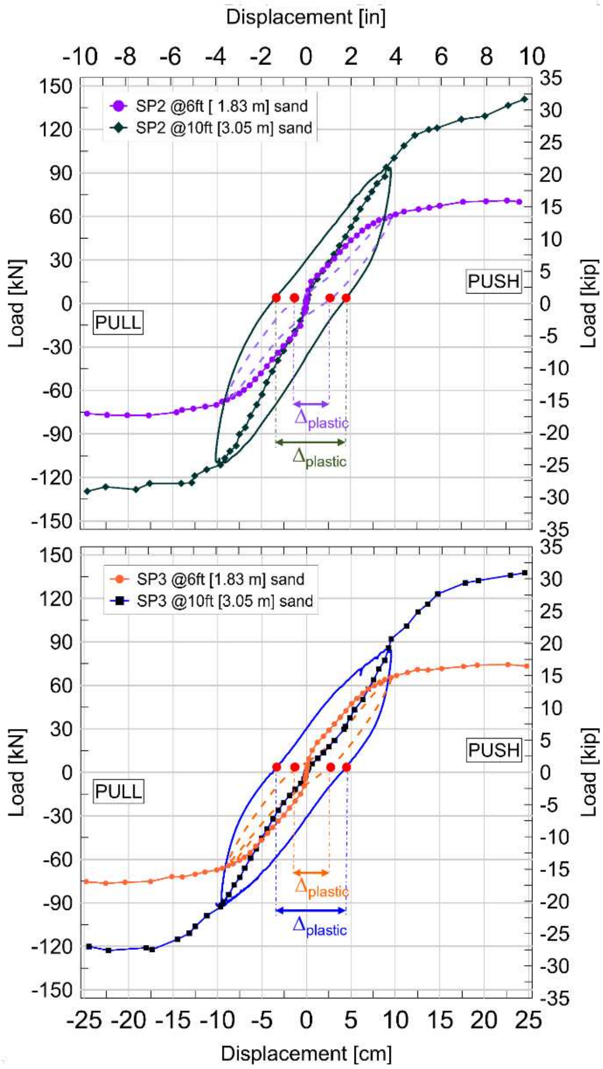

Figure 8. Experimental load-displacement backbone curves of Specimens 2 and 3.

Pile deformation profiles at selected pile head displacement levels are shown in Figure 9. The deformation profiles were recorded with inclinometer instrumentation and recorded during Phase 1 and Phase 2 testing. A comparison of Specimen 2's deformed shapes indicates that the plastic hinge has shifted and extended to a higher elevation by about 1.5 ft [0.45 m].

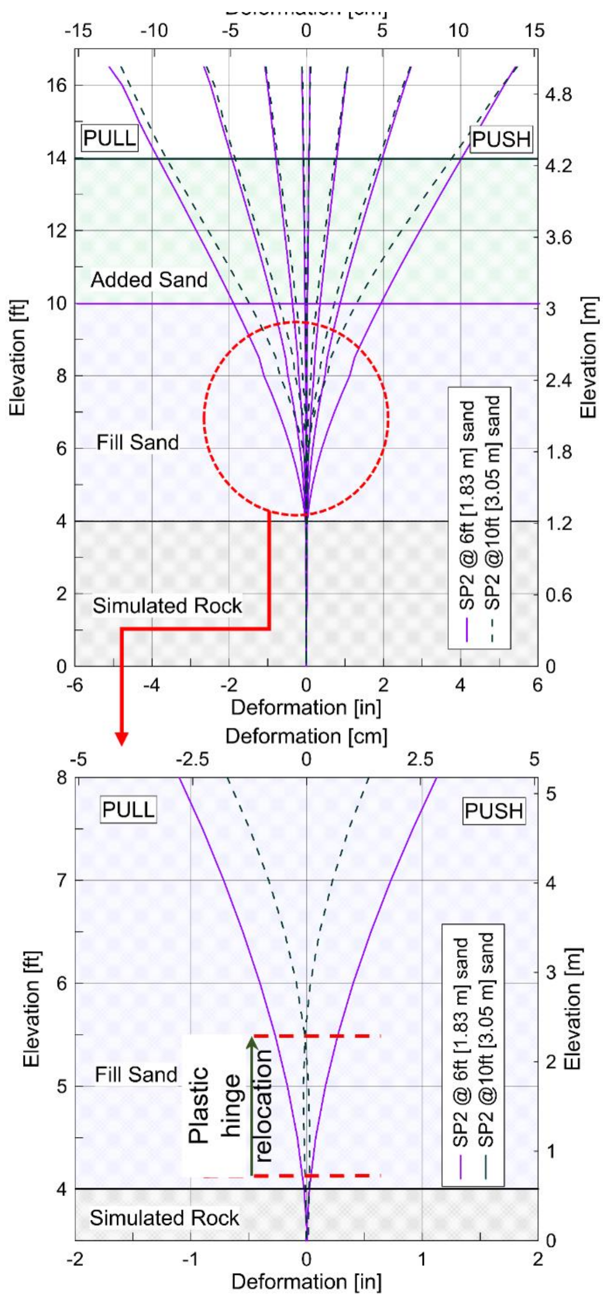

Figure 9. Deformed shape of Specimen 2 at selected applied displacement levels (inclinometer readings) after the initial testing in comparison with the after the retesting.

4 CONCLUSIONS

Large-scale lateral load testing was performed on two 18inch [45.7 cm] diameter pile specimens. Following initial testing of both specimens to complete structural failure, the soil stratigraphy was modified by raising the surcharge materials to strategically shift the initially developed plastic hinge to a higher elevation and to provide additional confinement around the pile specimens during retesting. Based on the experimental results, the following conclusions can be drawn:

- By adding a 4ft [1.2 m] thick soil layer, the initial stiffness of the failed piles was recovered by 100% for Specimen 2 and by 60% for Specimen 3.

- The transverse reinforcement ratio substantially influenced its ability to restore the initial pile stiffness but had less contribution to recovering the ultimate pile capacity.
- The proposed increase of the soil stratigraphy increased the ultimate pile capacity of Specimens 2 and 3 by an average of 80% and 70%, respectively.
- The ductility and energy dissipation of the retested piles improved greatly as a result of extending/relocating the pre-existing plastic hinge rather than introducing repairs to the plastic hinge region.
- Despite different transverse reinforcement ratios, Specimens 2 and 3 reached the same level of ductility during Phase 2 testing, which can be attributed to the confinement provided by the increase in sand surcharge.
- Findings of this specific experimental study showed that modifications to the soil stratigraphy around the pile upon partial or full loss of structural pile integrity could provide temporary increase and partial recovery of pile-soil capacity.

5 ACKNOWLEDGEMENTS

The experimental work was funded through DFI's Committee project fund, as well as through Prof. Lemnitzer's NSF funding (CMMI 1752303), along with generous industry support from our colleagues at DFI and ADSC. We would like to gratefully acknowledge the members of the DFI Drilled Shaft Committee, many of whom provided continuous feedback and guidance during the design and construction process [specifically Committee Chair Paul Axtell (Dan Brown and Associates), Peter Faust (Malcolm Drilling), Dr. Eric Loehr (Univ. of Missouri), and Dr. Armin Stuedlein (Oregon State University)]. We are furthermore extremely grateful for the material and equipment donations as well as the engineering support by: PJ Rebar (Nathan King), Atlas Geofoam (Chris Franks), Williams Form Engineering (Pete Speier and Jeff Ohlsen), Foundation Technologies, Inc. (Nick Milligan) and Gregg Drilling and Testing (Brian Savela and Kelly Cabal). Without the support of these colleagues, this research program would not have been possible in the scope described.

6 REFERENCES

American Society of Civil Engineers (ASCE). (2017). “Seismic evaluation and retrofit of existing buildings”, ASCE/SEI 41-17, Reston, VA.

ASTM C39 / C39M-21, Standard Test Method for Compressive Strength of Cylindrical Concrete Specimens, ASTM International, West Conshohocken, PA, 2021, www.astm.org

ASTM D1557-12e1. (2012) “Standard Test Methods for Laboratory Compaction Characteristics of Soil Using Modified Effort (56,000 ft-lbf/ft3 (2,700 kN-m/m3))”. ASTM International, West Conshohocken, PA, www.astm.org

ASTM D3080 / D3080M-11. (2011). “Standard Test Method for Direct Shear Test of Soils Under Consolidated Drained Conditions”. ASTM International, West Conshohocken, PA, www.astm.org.

Budek, A., Benzoni, G., & Priestley, M. J. (1994). In-Ground Plastic Hinges in Column/Pile Shaft Design. Proceedings, 3rd Annual Caltrans Seismic Research Workshop (p. 9). Sacrament, CA: California Department of Transportation, Division of Structures.

Chai, Y. H. and Hutchinson, T. C. (2002), "Flexural Strength and Ductility of Extended Pile-Shafts - Experimental Study", *Journal of Structural Engineering*, ASCE, 128(5), pp. 595-602.

Farrag, R., Cox, C., Turner, B., and Lemnitzer, A. (2020). Shear demands of rock-socketed piles subject to cyclic lateral loading. *DFI Journal - The Journal of the Deep Foundations Institute*,14 (2), https://doi.org/10.37308/DFIJnl.20200526.223

Priestley, M. J., Seible, F., & Calvi, G. M. (1996). Seismic Design and Retrofit of Brdiges. New York: John Wilen and Sonces, Inc.